International Journal of Multiphysics
Volume 19, No. 1, 2025
ISSN: 1750-9548

Design and Analysis of a flexible and optically transparent of Multi-Band Absorber with Polarization Insensitivity for conformal applications

Alireza Bayat *[1], Reza Mirzakhani[2]

[1] *PhD degree, Faculty of Technical and Engineering, Electrical Engineering-Telecommunication, Imam Khomeini International University, Qazvin, Iran
abaiat@eng.ikiu.ac.ir *Corresponding author

[2]Ph.D Candidate, Faculty of Technical and Engineering, Electrical Engineering-Telecommunication, Imam Khomeini International University, Qazvin, Iran.

reza.mirzakhani@edu.ikiu.ac.ir.

Abstract

This study presents the design and analysis of a multi-band, optically transparent metamaterial absorber (MA) based on a 5×5 array of unit cells, bent by 90 degrees to investigate its electromagnetic response over a frequency range of 0 to 25 GHz. The absorber is constructed using indium tin oxide (ITO) and polyethylene terephthalate (PET) films on a polyvinyl chloride (PVC) substrate, achieving high absorption efficiency across multiple frequency bands. Characteristic Mode Analysis (CMA) is applied to optimize the resonant behavior of cross-shaped and ring-shaped resonators, while accounting for the effects of bending on surface current distribution and modal coupling. Surface current distribution is thoroughly analyzed for the bent structure, revealing significant changes in resonant behavior compared to the flat configuration. The absorption characteristics are compared across different incident angles (0°, 15°, 30°, and 45°), with the results showing shifts in resonant frequency and absorption efficiency. Although absorption remains high at normal incidence, predictable degradation is observed at higher angles. The study provides key insights into the design of flexible, broadband absorbers for applications requiring transparency and angular stability, such as electromagnetic interference (EMI) shielding and stealth technology. This MA offers a promising solution for optoelectronic devices, with potential for further optimization to improve angular performance.

Keywords: Circuit analog absorbers, characteristic mode analysis, indium tin oxide, electromagnetic shielding, oblique incidence

.Introduction

Metamaterial absorbers (MAs) have emerged as revolutionary materials capable of manipulating electromagnetic waves in ways that conventional materials cannot. They are particularly effective in absorbing electromagnetic radiation, thereby reducing radar cross sections (RCS) and mitigating electromagnetic interference (EMI). This ability to control electromagnetic waves has significant implications for stealth technology, electromagnetic shielding, and various optoelectronic applications. Traditionally, MAs are opaque, limiting their utility in scenarios where optical transparency is essential, such as in electromagnetic shielding for windows, transparent displays, and various optoelectronic devices[1]. In recent work, a novel metamaterial absorber using ITO and polymethyl methacrylate (PMMA) has been proposed. This absorber achieves greater than 90% absorption in the 5.7–16.4 GHz range and over 70% light transmittance. The design is guided by radiation–absorption reciprocal theory and characteristic mode analysis, ensuring high performance and robustness under varying conditions [1].

Recent advancements in materials science have led to the development of optically transparent metamaterials. Indium tin oxide (ITO), a widely used N-type oxide semiconductor, has gained attention due to its high optical transparency, high carrier concentration, and low resistivity[1]. Several studies have explored the use of ITO in the design of transparent MAs[1-8]. For instance, Zhang et al. [7] demonstrated a high-performance broadband electromagnetic interference shielding optical window using an ITO-based metamaterial absorber. However, these designs often face challenges such as limited bandwidth, sensitivity to the angle of incidence, and reduced optical transmittance. to address these limitations, various methods have been proposed. One approach involves the use of multilayer structures to enhance bandwidth and absorption efficiency. For example, Deng et al. [4] designed an ultra-broadband optically transparent MA by stacking multilayer ITO films, achieving high absorption over a wide frequency range but at the cost of reduced optical transmittance . Another approach utilizes composite structures to achieve multi-resonance modes, enhancing absorption across multiple frequency bands while maintaining high optical transparency.

A notable advancement in this field is the development of an optically transparent flexible metamaterial structure that achieves high absorptivity in the frequency ranges of 33.7-44.7 GHz for TE polarization and 11.8-37.2 GHz for TM polarization. This structure is designed by modifying the impedance and resonance peaks of the meta-atom, demonstrating practical applications in multispectral stealth technology. The design maintains high performance across a wide incident angle of ±60° [6].

Further innovations include the creation of a double-layer coupled broadband absorbing metamaterial with optical transparency characteristics. This absorber features a ring indium tin oxide (ITO) resonant unit and achieves ultra-wideband microwave absorption between 5.2 GHz and 18 GHz with a low-profile structure of only 6 mm. The materials used exhibit good optical transparency, making the absorber suitable for various applications requiring both EM absorption and transparency [2].

Another significant contribution is the development of a visible transparent wideband microwave absorber with infrared camouflage function. This absorber integrates radar absorption layers and an infrared shielding layer, achieving absorption rates greater than 90% across 7-23 GHz. It also features an average visible transmittance of ~60%, offering practical applications in multispectral stealth environments [3].

Additionally, a highly visible to near-infrared (Vis-NIR) transparent metamaterial window has been developed, featuring excellent microwave broadband absorption and practical durability. This window uses a sandwich structure with cross-ring resonators and a reflective backplane, achieving over 80% absorptivity in the 6.6-13.8 GHz range and maintaining high optical transmittance. The material also shows excellent environmental resistance and durability [8].

The demand for advanced electromagnetic (EM) wave absorbers that combine high efficiency with optical transparency has driven significant research and development in the field of metamaterials. Traditional microwave absorbers are effective in reducing radar cross-sections and minimizing electromagnetic interference, but they are typically opaque and unsuitable for applications where visibility is crucial. This limitation has spurred the development of optically transparent wideband metamaterial absorbers, which offer the dual benefits of EM wave absorption and light transmittance, thus extending their applicability to specialized environments such as anechoic chamber glass, cockpit glass, and other transparent surfaces in stealth technology.

This study aims to design and analyze a novel multi-band metamaterial absorber (MA) that achieves high optical transparency and polarization insensitivity. The specific objectives are:

1. To design a metamaterial structure that combines cross-shaped and ring-shaped resonators for multi-band absorption.

2. To utilize characteristic mode analysis (CMA) and equivalent circuit models to optimize the absorber’s performance across multiple frequency bands.

3. To validate the absorber’s performance through numerical simulations, focusing on its absorption efficiency, polarization insensitivity, and optical transparency.

The development of a multi-band, optically transparent MA with polarization insensitivity has significant implications for various applications. In stealth technology, such absorbers can enhance the stealth capabilities of vehicles and structures without compromising visibility. In electromagnetic interference shielding, they can protect sensitive electronic equipment while allowing light to pass through, making them ideal for use in windows and transparent displays. Additionally, in optoelectronic devices, these absorbers can improve device performance by mitigating electromagnetic interference without affecting optical functionality. The proposed design not only addresses the limitations of existing transparent MAs but also opens new avenues for their application in advanced technological fields.

1. Design Methodology

2-1- Material Selection

In designing a multi-band, optically transparent metamaterial absorber (MA), the choice of materials is crucial for achieving desired electromagnetic properties while maintaining high optical transparency. This study employs indium tin oxide (ITO) and polyethylene terephthalate (PET) films, combined with a polymethyl methacrylate (PMMA) substrate, due to their unique properties that collectively enhance the performance of the MA. ITO is a widely recognized material for its excellent optical transparency and electrical conductivity. It is composed of indium oxide ($In_2 O_3$) and tin oxide (SnO_2) in varying proportions, typically 90% $In_2 O_3$ and 10% SnO_2. The high carrier concentration in ITO results in low resistivity, making it ideal for applications requiring both transparency and conductivity. ITO films can achieve an optical transmittance of up to 90% in the visible spectrum, making them suitable for applications where maintaining visibility is crucial. the low resistivity of ITO, typically in the range of 10^{-4} to 10^{-3} Ω·cm, allows it to efficiently conduct electrical currents, which is essential for the resonant properties of metamaterial absorbers [4, 7, 9-13].

ITO exhibits a high plasma frequency (ω_p), typically in the near-infrared region, which contributes to its effectiveness in manipulating electromagnetic waves in the microwave to terahertz frequency range. The plasma frequency can be described by the equation:

$$\omega_p = \sqrt{\frac{ne^2}{\varepsilon_0 m^*}} \quad (1)$$

where (n) is the carrier concentration, (e) the electron charge, (ε_0) is the permittivity of free space, and (m*) is the effective mass of the carriers.

PET is a widely used thermoplastic polymer known for its excellent mechanical properties and optical clarity. When used as a substrate or as part of a composite structure in MAs, PET provides several benefits:

Mechanical Strength: PET is durable and resistant to impact, which helps maintain the structural integrity of the MA.

Optical Clarity: PET films can achieve high optical transparency, complementing the transparency provided by ITO.

Flexibility: PET is flexible, allowing for the fabrication of flexible MAs that can conform to various surfaces and shapes[14].

PMMA, also known as acrylic or plexiglass, is another optically transparent material used as the substrate in this study. PMMA is chosen for its superior optical properties and ease of fabrication:

High Optical Transmittance: PMMA can transmit up to 92% of visible light, which is critical for maintaining the transparency of the entire MA structure[15].

Low Dielectric Constant: PMMA has a low dielectric constant ($\varepsilon_r \approx 2.6 - 3.3$), which minimizes dielectric loss and enhances the efficiency of electromagnetic wave absorption[16]. The dielectric constant influences the propagation of electromagnetic waves and can be described by the equation:

$$\varepsilon_r = \epsilon' - j\epsilon'' \quad (2)$$

where (ϵ') is the real part (dielectric constant) and (ϵ'') is the imaginary part (dielectric loss). PMMA is thermally stable up to about 160°C, making it suitable for applications that may involve varying temperatures[17].

The electromagnetic properties of the materials used are fundamental to the performance of the MA. ITO's high conductivity and plasma frequency enable effective interaction with electromagnetic waves, facilitating the creation of resonant modes necessary for absorption. PET and PMMA, with their low dielectric constants and high optical transparency, ensure that the structure remains transparent while supporting the resonant behavior of the ITO layers [15]. The combination of these materials results in a metamaterial absorber that can effectively absorb electromagnetic waves across multiple frequency bands while maintaining high optical transmittance.

Looking forward, the development of advanced materials such as graphene and other two-dimensional materials holds promise for further enhancing the performance of optically transparent MAs. Graphene, for instance, offers exceptional electrical conductivity, mechanical strength, and optical transparency, making it an ideal candidate for next-generation metamaterial absorbers. Additionally, the exploration of novel composite materials and hybrid structures could lead to even more efficient and versatile MAs with applications extending into higher frequency ranges and more demanding environments[14].

2-2- Structural Design

In the development of a multi-band, optically transparent metamaterial absorber (MA), the structural design plays a critical role in determining the absorber's efficiency and bandwidth. This section outlines the key design considerations and methodologies employed in structuring the MA to achieve optimal performance. The design methodology involves integrating exponentially tapered cross-shaped and ring-shaped resonators to achieve multi-band absorption[5]. The exponentially tapered structure leverages the unique properties of indium tin oxide (ITO) and polyethylene terephthalate (PET) films, combined with a Polyvinyl Chloride (PVC) substrate, to maintain high optical transparency and effective electromagnetic absorption. The exponentially tapered shaped resonators are incorporated in the design to facilitate multi-band absorption. These resonators are known for their ability to create multiple resonant modes within the desired frequency range, enhancing the bandwidth and efficiency of the MA.

Optimization: The optimization of the cross-shaped resonators involves adjusting their geometric parameters to maximize absorption at target frequencies while maintaining optical transparency. This includes refining the length, width, and spacing of the resonator arms to achieve the desired resonant behavior [5].

2-3- Characteristic Mode Analysis

Characteristic Mode Analysis (CMA) is a powerful method used to analyze and optimize the resonant behavior of the proposed metamaterial absorber (MA). CMA provides a systematic approach to evaluate the modal significance of the resonators and predict their resonant frequencies, ensuring efficient absorption across the desired frequency range. CMA is based on the theory of characteristic modes, which was first proposed by Garbacz in 1965 [18]. This theory involves solving for the eigenvalues and eigenvectors of the current distribution on a perfectly conducting surface. The characteristic modes are defined as the eigenfunctions of the associated operator, and they provide valuable insights into the resonant behavior of the structure. The characteristic modes are solutions to the eigenvalue problem:

$$[X]\boldsymbol{J}_n = \lambda_n[R]\boldsymbol{J}_n \quad (3)$$

where [X] and [R] are the reactance and resistance matrices, respectively, λ_n are the eigenvalues, and J_n are the eigenvectors representing the characteristic currents [18]. The modal significance (MS) is a key parameter in CMA, defined as:

$$MS = \frac{1}{1+j\lambda_n} \quad (5)$$

where λ_n is the eigenvalue corresponding to the n-th mode. MS indicates how close a mode is to resonance, with values close to 1 indicating strong resonance [18]. Modes with high modal significance are targeted for optimization to enhance overall performance [7].

The radiation patterns of the characteristic modes are analyzed to ensure efficient absorption of electromagnetic waves. The distribution of surface currents and the resulting electromagnetic fields are studied to understand how the absorbed energy is dissipated. Modes with desirable radiation patterns are selected to maximize the absorber's efficiency [19]. In the design of the proposed MA, CMA is used to identify and optimize the resonant modes of the cross-shaped and ring-shaped resonators. The analysis involves the following steps:

Calculation of Modal Significance: The modal significance of each resonator is calculated to identify the effective resonant modes that contribute to absorption. Modes with high MS are selected for further optimization [20]

Optimization of Resonator Dimensions: The dimensions of the resonators are adjusted to tune the resonant frequencies to the desired bands. This involves iterative simulations and adjustments to achieve the optimal configuration[21].

Analysis of Combined Structure: The cross-shaped and ring-shaped resonators are combined, and the characteristic modes of the entire structure are analyzed. This ensures that the combined structure provides broad bandwidth and high efficiency [22].

Numerical simulations are performed using CST Microwave Studio [23] to validate the results of the CMA. The simulations provide detailed insights into the electromagnetic behavior of the MA, allowing for iterative refinement of the design. The simulation results are used to verify the modal significance, radiation patterns, and overall absorption efficiency of the proposed MA [24].

Bending the structure introduces curvature, which affects the distribution of surface currents and the resulting electromagnetic fields. This curvature can lead to the coupling of modes that would otherwise be isolated in a flat configuration, potentially leading to new resonances or modifying existing ones. CMA is being used to analyze these effects by solving for the characteristic modes on the curved surface.

Mode Coupling and Hybridization: The bending of the array can lead to the hybridization of characteristic modes, where two or more modes combine to form a new mode with different properties. This hybridization can either broaden the absorption bandwidth or shift the resonant frequencies, depending on the degree of coupling and the specific geometry of the bend.

Curved Surface Analysis: The analysis of characteristic modes on a curved surface requires modifications to the standard CMA approach. The eigenvalue problem is still solved in the same manner, but the boundary conditions and the geometry of the surface must be adjusted to account for the curvature. The modal significance (MS) in this context might differ from that of a flat structure, and additional modes might be excited due to the curved geometry.

Modified Surface Currents and Boundary Conditions

When the structure is bent by 90 degrees, the distribution of surface currents on the unit cells is altered due to the change in geometry. In a flat structure, surface currents **J®** are typically distributed based on the uniform boundary conditions across the flat plane. However, bending introduces curvature, modifying the boundary conditions along the curve. Let's denote the position vector in the curved structure as $\mathbf{r}'$. The new surface current distribution $\mathbf{J}'(\mathbf{r}')$ can be expressed as:

$$\mathbf{J}'(\mathbf{r}')=\mathbf{J}(\mathbf{r})\cdot\mathbf{T}(\theta) \quad (6)$$

where $\mathbf{T}(\theta)$ is the transformation matrix accounting for the bending angle θ, and $\mathbf{r}'$ represents the position on the curved surface. For a 90-degree bend, $\theta=\pi/2$ radians.

Eigenvalue Problem on a Curved Surface

The characteristic modes in a flat structure are solutions to the eigenvalue problem:

$$[X]\mathbf{J}_n=\lambda_n[R]\mathbf{J}_n \quad (7)$$

where [X] is the reactance matrix, [R] is the resistance matrix, λ_n are the eigenvalues, and $\mathbf{J}_n$ are the characteristic currents [18]. For a bent structure, the geometry modifies the eigenvalue problem. The curvature can be represented by a change in the coordinates and corresponding differential operators. The eigenvalue equation on the curved surface becomes:

$$[X']\mathbf{J}'_n=\lambda'_n[R']\mathbf{J}'_n \quad (8)$$

where [X′] and [R′] are the modified reactance and resistance matrices for the curved geometry. The eigenvalues λ'_n and eigenvectors $\mathbf{J}'_n$ reflect the impact of bending on the characteristic modes.

Mode Coupling and Hybridization

Bending can cause adjacent modes that are uncoupled in a flat configuration to couple, leading to hybridization of modes. This coupling can be represented as an interaction term in the characteristic mode equation. Let $\mathbf{J}_m$ and $\mathbf{J}_n$ be two characteristic modes that couple due to bending. The coupled modes can be expressed as a linear combination:

$$\mathbf{J}_{m+n}=\alpha\mathbf{J}_m+\beta\mathbf{J}_n \quad (9)$$

where α and β are coefficients determined by the degree of coupling induced by the bending. The new eigenvalue equation incorporating this coupling is:

$$([X]+[\Delta X])(\alpha\mathbf{J}_m+\beta\mathbf{J}_n)=(\lambda+\Delta\lambda)([R]+[\Delta R])(\alpha\mathbf{J}_m+\beta\mathbf{J}_n) \quad (10)$$

where [ΔX] and [ΔR] are the perturbations to the reactance and resistance matrices due to bending.

Impedance Matching on Curved Structures

The bending of the structure also affects the input impedance of the array. For a flat structure, the input impedance Zin is matched to the free space impedance $Z_0=377\,\Omega$ to maximize absorption. However, bending alters the impedance, which must be recalculated. The input impedance for the bent structure can be expressed as:

$$Z'_{in}(\theta)=Z_{in}\cdot f(\theta) \quad (11)$$

where f(θ) is a function describing the change in impedance due to bending. For a 90-degree bend (θ=π/2), f(θ) accounts for the curvature and any associated reflection or transmission losses.

Radiation Patterns and Far-Field Effects

Bending also modifies the far-field radiation patterns of the characteristic modes. In a flat structure, the far-field radiation pattern $\mathbf{E}(\theta,\phi)$ is determined by the Fourier transform of the surface currents. In a bent structure, the radiation pattern is altered due to the change in surface current distribution:

$$\mathbf{E}'(\theta,\phi)=F\{\mathbf{J}'(\mathbf{r}')\} \quad (12)$$

where F denotes the Fourier transform, and $\mathbf{r}'$ is the position vector on the curved surface.

3- Numerical Simulation and Results

Numerical simulations, such as those performed in CST Microwave Studio[23], are essential for verifying the theoretical predictions made using CMA. Simulations allow for the visualization of surface current distributions and absorption characteristics of the bent 5×5 array. The simulation accurately models the bent structure, including the curvature and array configuration. Special attention must be paid to boundary conditions and mesh settings to ensure that the curvature is properly resolved. Comparing the results of the bent array with a flat array can provide insights into how bending affects the performance. Differences in absorption efficiency, bandwidth, and resonant frequencies should be analyzed to guide further optimization. In this section, we will explain the scan angles for unit cell or periodic boundary conditions. These settings are supported by the frequency domain solver. Since the frequency domain solver calculation is performed and waveguide ports share one or two pairs of edges with periodic boundaries, the phase shift and constant angle of incidence definitions affect the port modes. For instance, if a constant angle of incidence is specified, homogeneous ports with periodic boundaries yield a plane wave

propagating along the direction given in spherical coordinates (theta and phi), and a number of higher-order Floquet modes.

if activated, you may enter an angle modifying the phase on the periodic boundaries. The periodic phase shift is changed across the periodic boundaries according to the phase value of an imaginary incident plane wave at the boundaries with the angles theta and phi.

Theta is the angle between the z-axis and the propagation direction of a plane wave in background material.

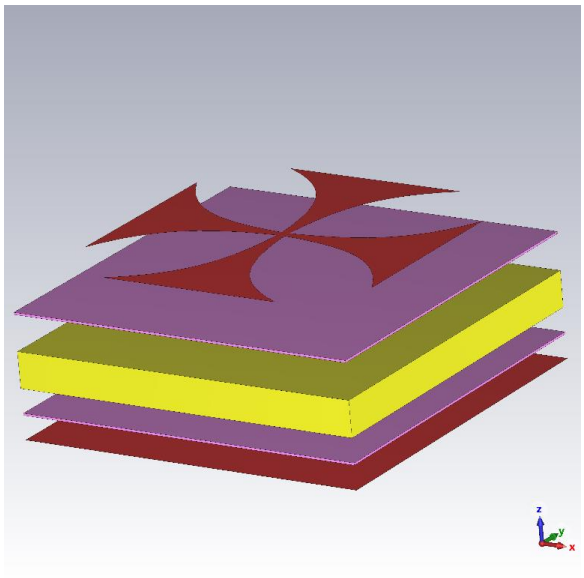

Figure 1 Explosive view of Designed unit cell

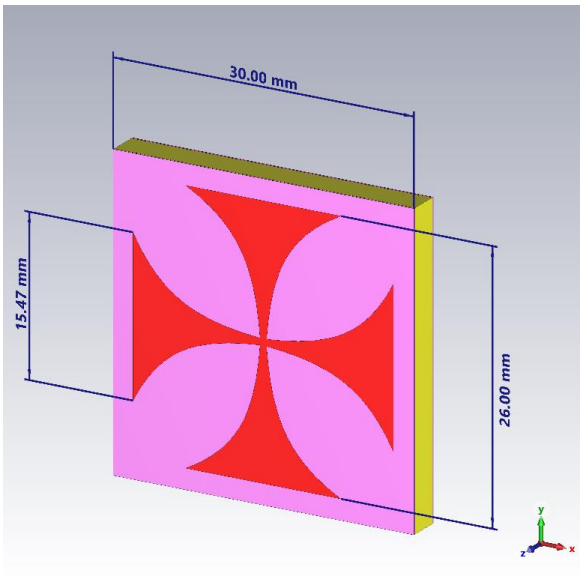

Figure 2 3D view of Designed unit cell

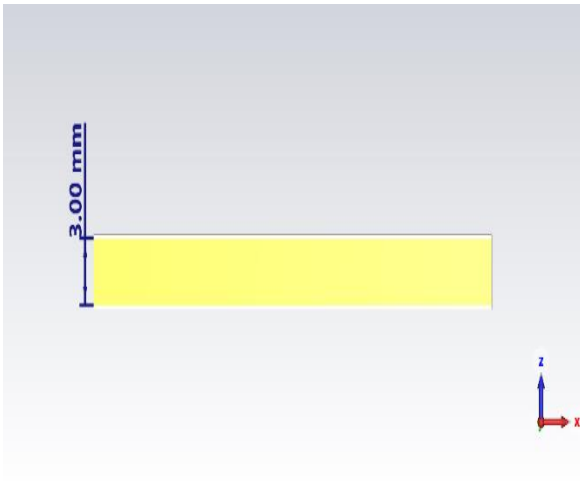

Figure 3 Side view of Designed unit cell

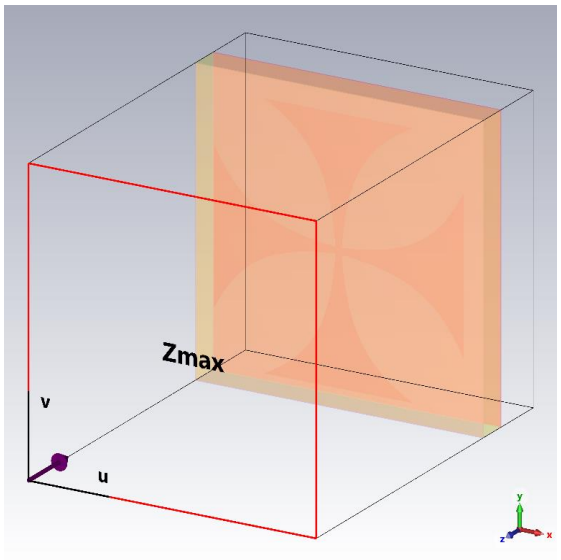

Figure 4 Floquet Z max port

The unit cell designed by the [5] shows very good bandwidth and was optimized, the designed unit cell has been modified the edge of absorbing layer exponentially [25] to achieve wider bandwidth. For reaching the desired result the width proposed unit cell introduced in [5] increased to 30 and is optimized by parametric study.

The array of 5×5 unit cell is considered to propose the conformal application of unit cell by bending the plane by 90 degree. The use of a 5×5 array of unit cells in the design of a metamaterial absorber enhances the absorber's performance by increasing the interaction area with incident electromagnetic waves. Arrays are commonly used in metamaterial designs to scale up the effects observed in single-unit cells, thereby improving the overall absorption efficiency. When this array is bent by 90 degrees, it introduces additional complexity into the electromagnetic behavior, particularly in how the characteristic modes are excited and how they interact with incident waves from different angles.

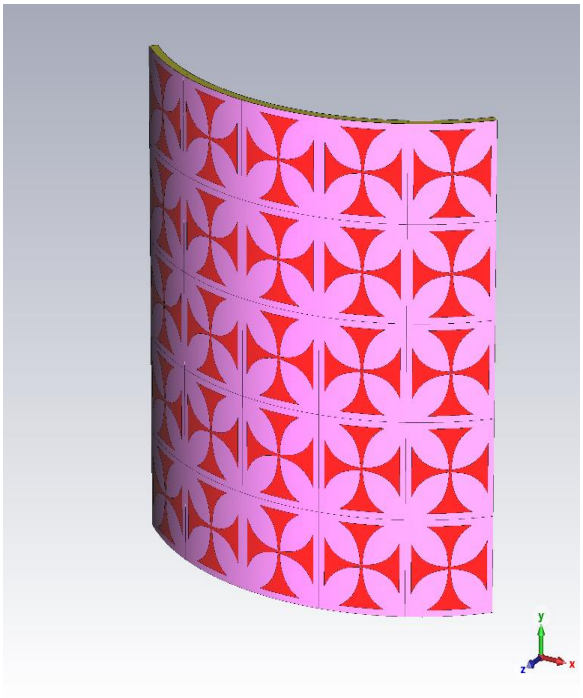

Figure 5 3D View of Array of 5*5 bent by 90 degrees

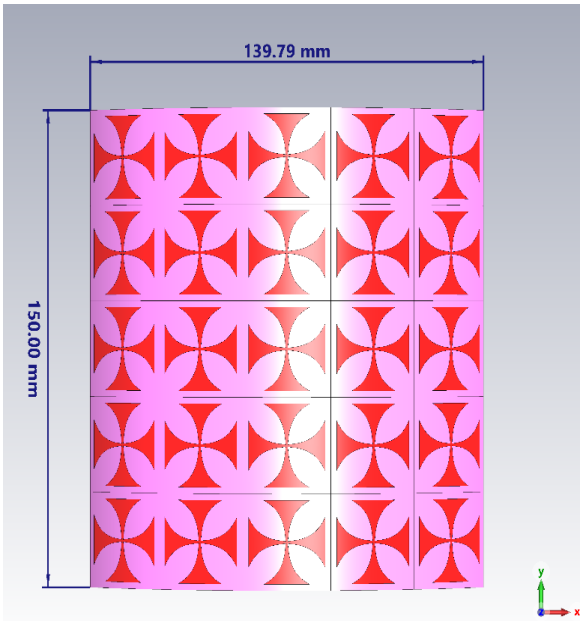

Figure 6 front View of Array of 5*5 bent by 90 degrees

The incident angle of electromagnetic waves significantly impacts the absorption characteristics of metamaterial absorbers. As the angle of incidence increases, the interaction between the incoming waves and the resonant structures (such as the unit cells in 5×5 array) changes, affecting the efficiency and bandwidth of absorption. At 0° incidence, the electromagnetic waves are perpendicular to the surface of the absorber. This is typically where the designed resonant modes are most effectively excited, leading to maximum absorption at the intended resonant frequencies. The electric and magnetic fields are optimally coupled with the resonators, leading to the strongest absorption peaks.

Oblique Incidence (15°, 30°, 45°): As the angle of incidence increases, the path length of the waves interacting with the unit cells becomes longer. This changes the effective electrical size of the resonators and can shift the resonant frequencies. Additionally, higher incidence angles can lead to a reduction in the coupling efficiency between the incident wave and the resonator modes, which might decrease the absorption magnitude or shift the absorption peak to a different frequency.

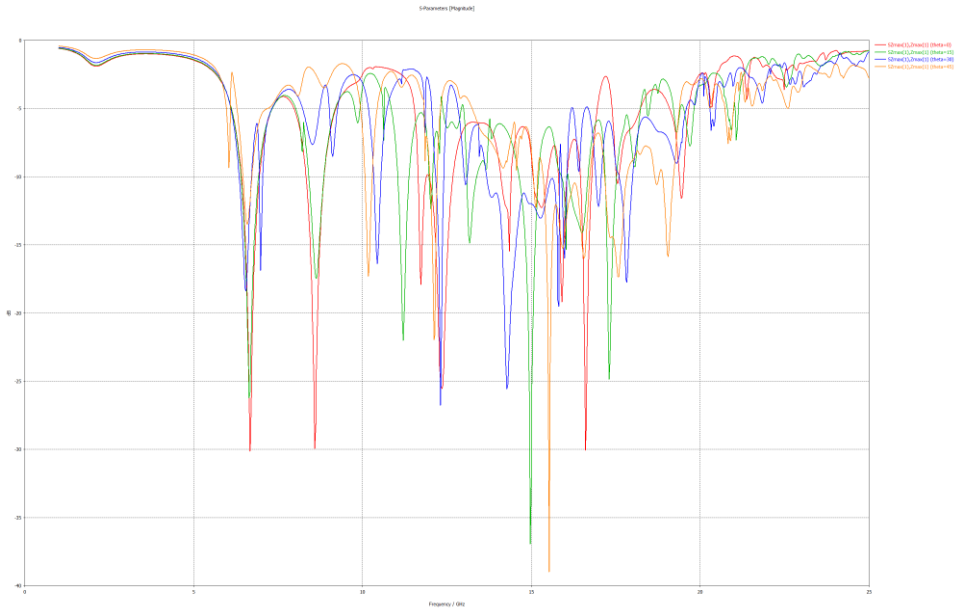

Figure 7 S11 at maximum side of unit cell in 0,15,30 and 45 degree of incident angle

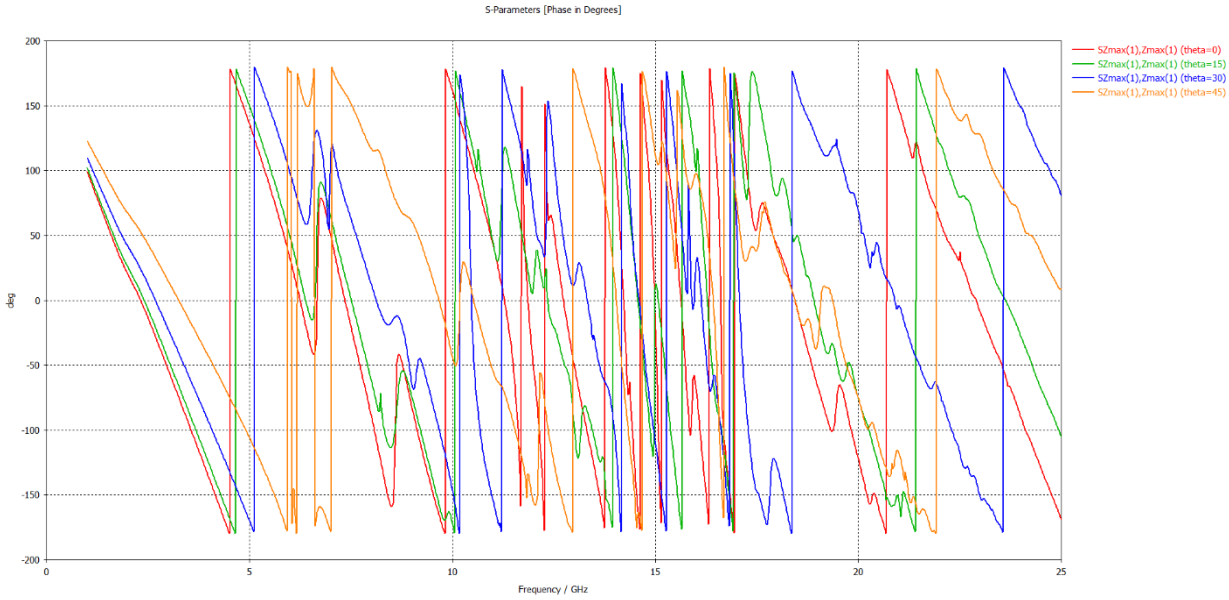

Figure 8 S-parameter of 0,15,30 and 45 phase degrees

4- Discussion

When comparing the results at 0°, 15°, 30°, and 45°, you can expect the following trends:

Shift in Resonant Frequency: As the angle increases, there may be a slight shift in the resonant frequencies. This is due to the change in the effective electrical length of the resonators as seen by the incident waves. The degree of this shift depends on the geometry and material properties of the resonators.

Decrease in Absorption Efficiency: Generally, the absorption efficiency tends to decrease as the incident angle increases. This is because the resonance condition becomes less effective as the waves approach more obliquely, leading to less energy being absorbed by the resonators. The absorption peaks may become broader and less pronounced.

Polarization Effects: Depending on whether the incident wave is TE (Transverse Electric) or TM (Transverse Magnetic) polarized, the absorption behavior might differ at oblique angles. TE waves typically experience greater changes in absorption characteristics with angle compared to TM waves due to the difference in how the electric field interacts with the resonators.

The simulation results provide data such as reflection (S11), transmission (S21), and absorption (A=1−|S11|2−|S21|2 A=1−|S11|2−|S21|2), you can plot these parameters for each incident angle to visually compare the performance.

At 0°, the absorption peak is at 6.664 GHz with 95% efficiency.

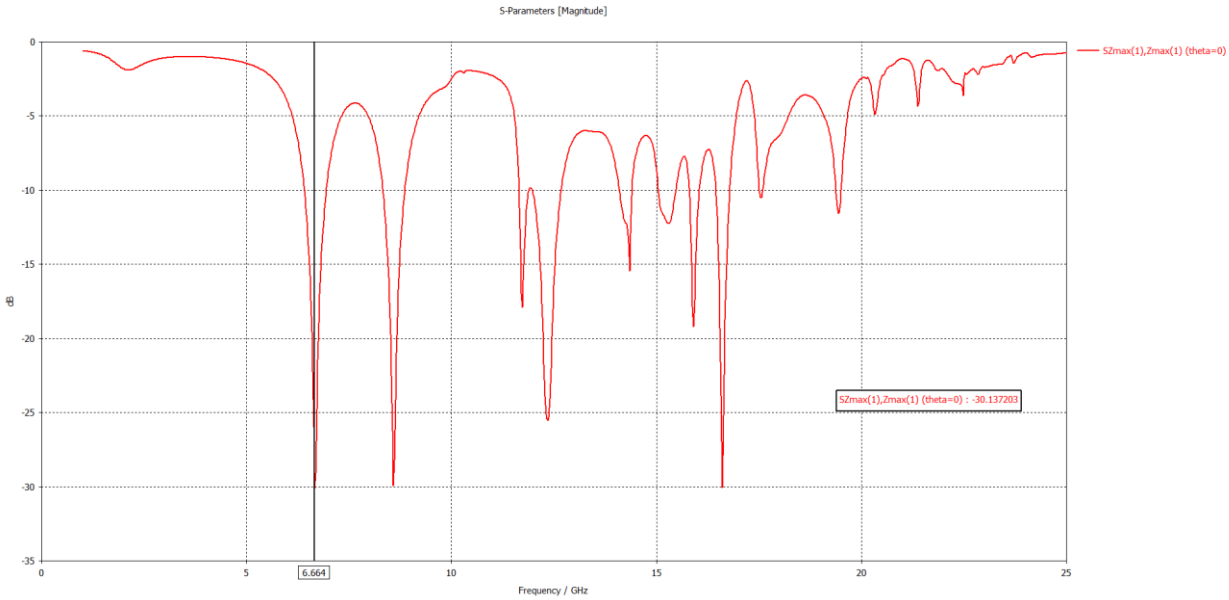

Figure 9 S-parameter of incident of 0 degree

At 15°, the peak shift slightly to upper range and new channel is opened at 14.968 GHz with -37 dB absorption with 95% efficiency.

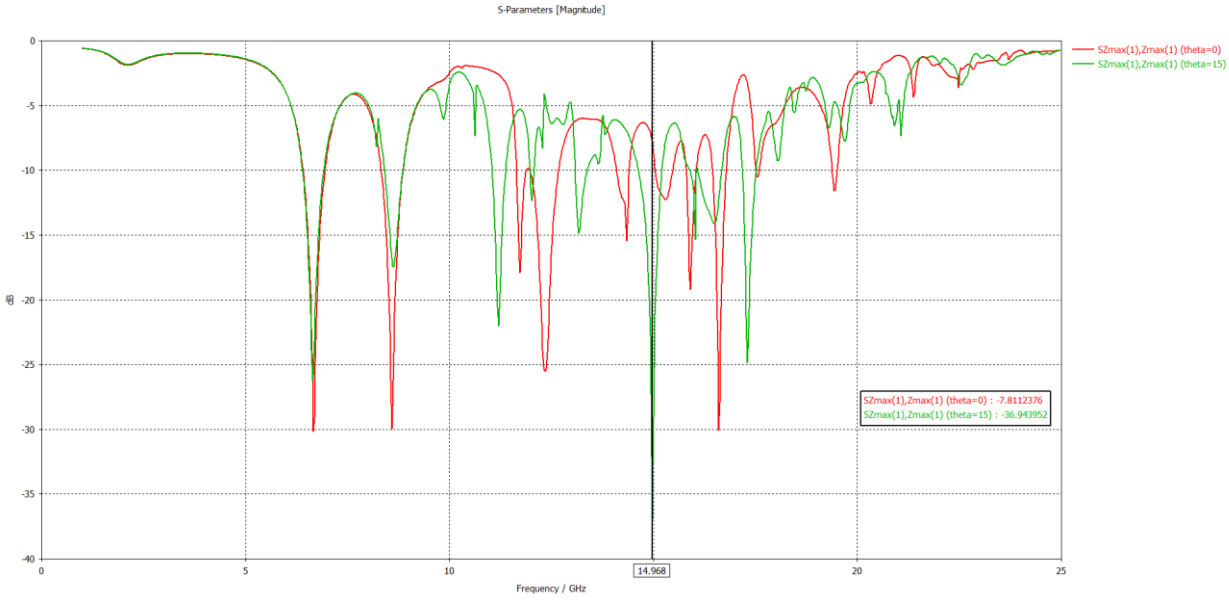

Figure 10 Comparison of 0-degree incident by 15 degrees

At 30°, the peak shift further to 10.5 GHz with 85% efficiency.

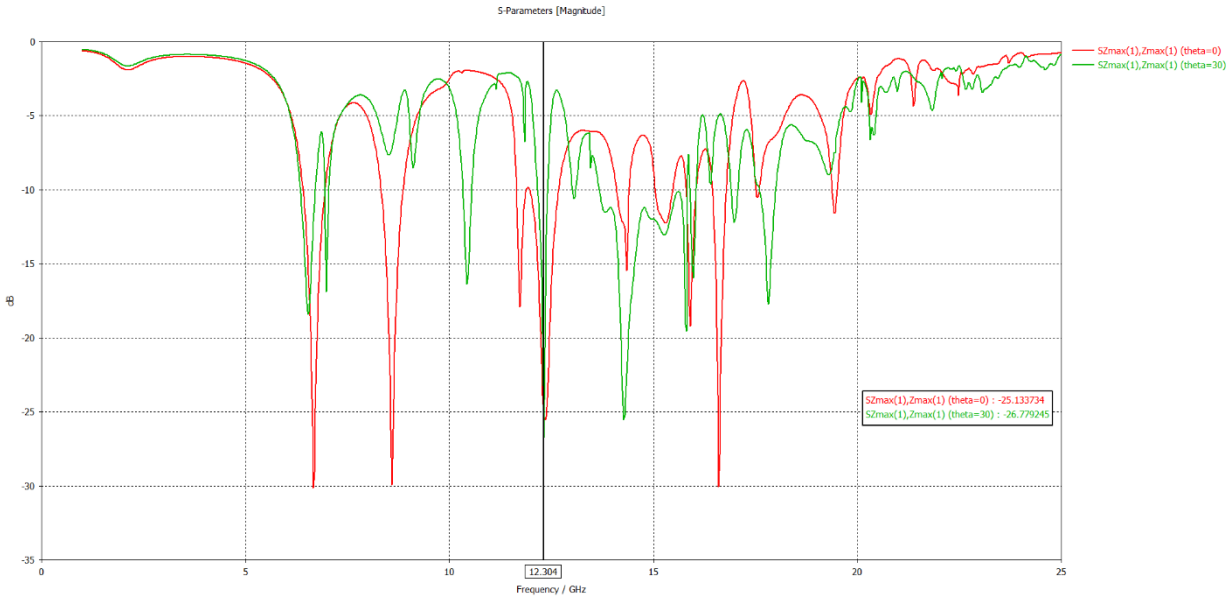

Figure 11 Comparison of 0 degree incident by 30 degree

At 45°, the peak broaden, the absorption chanenel is opened at 15.52 GHz with -39dB absorption and 98% efficiency.

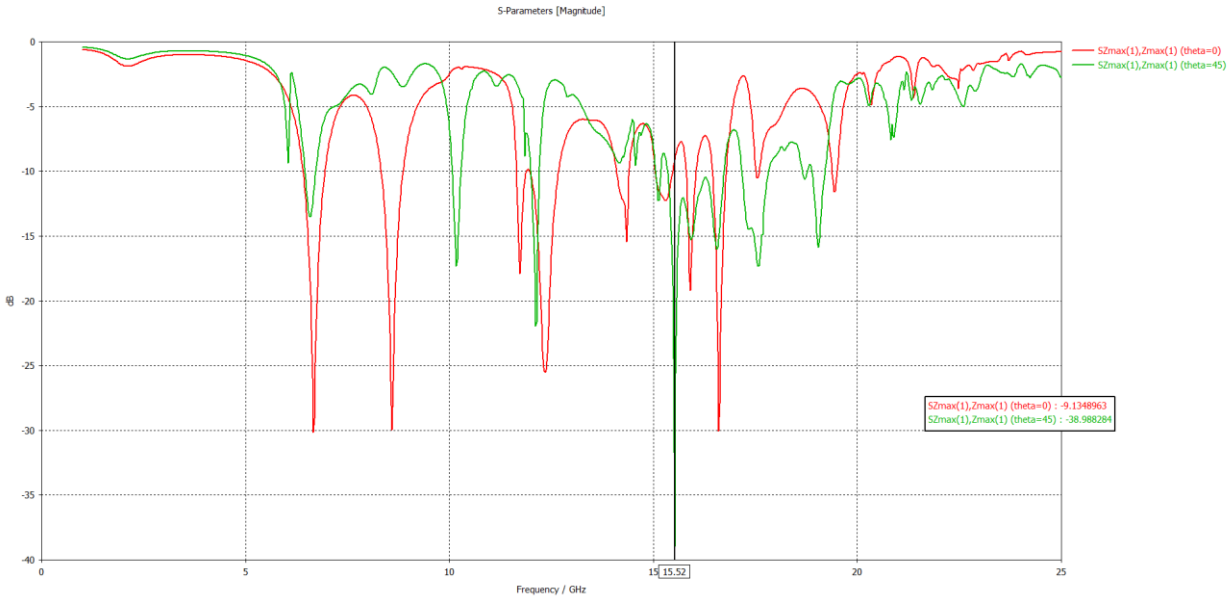

Figure 12 Comparison of 0-degree incident by 45 degrees

These observations depict that while the absorber is robust at normal incidence, its performance slightly degrades at higher angles, which is typical for many metamaterial absorbers.

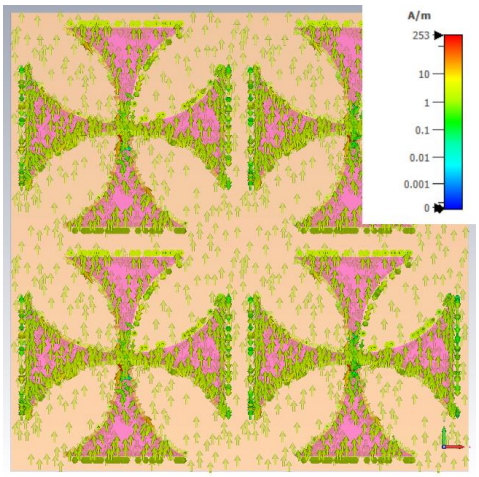

Figure 14 Surface current distribution at 1 Ghz

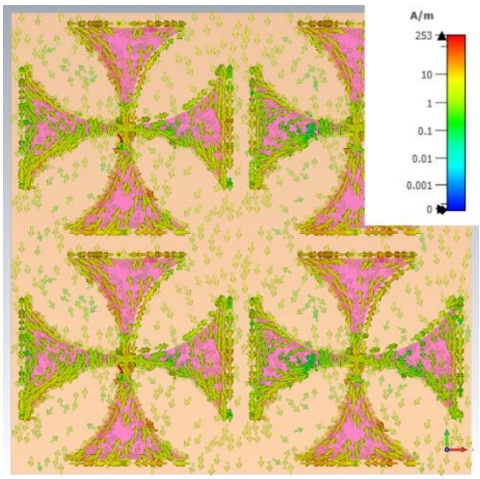

Figure 13 Surface current distribution at 13 Ghz

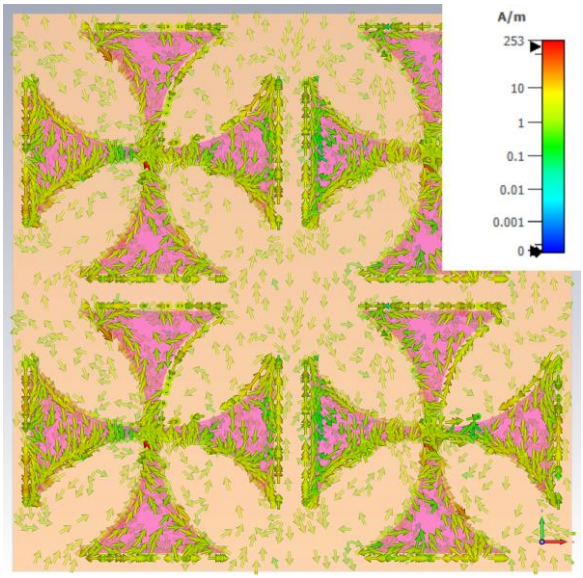

Figure 15 Surface current distribution at 25 Ghz

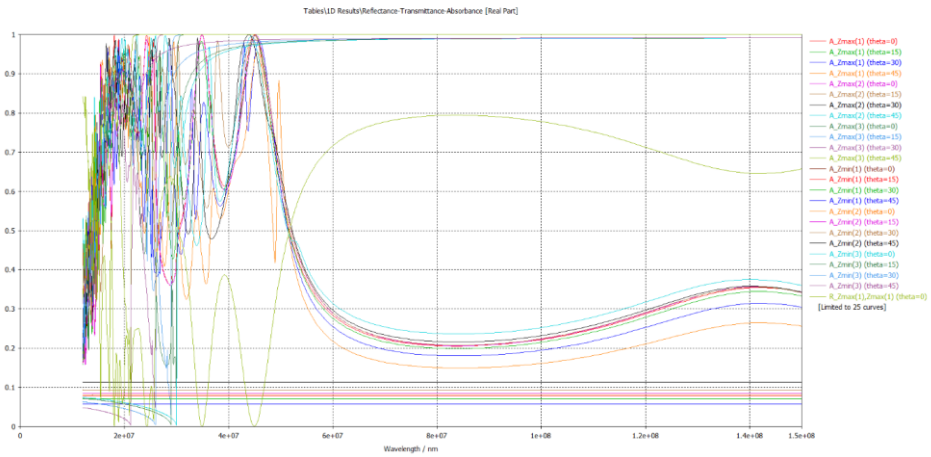

Figure 16 Reflection, Transmittance and Absorption

5- Conclusion

Simulating exponentially modified CA absorber at multiple incident angles is an essential step in understanding its real-world performance. The insights gained from these simulations can guide further optimization to ensure that the absorber performs effectively across a wide range of angles, making it suitable for more practical applications. If significant performance degradation is observed at higher angles, you might consider optimizing the design further. Possible by Modifying the geometry to make the resonators less sensitive to incident angle. also Introducing multi-resonance structures can help maintain high absorption over a wider range of angles.by Using gradient-index layers can help mitigate reflection and improve impedance matching at higher angles. Bending a 5×5 array of unit cells by 90 degrees introduces significant changes to the characteristic modes, including modifications to the surface currents, coupling of modes, and changes in impedance and radiation patterns. These effects can be quantitatively analyzed using the modified eigenvalue equations and considering the impact of curvature on the characteristic mode parameters.

REFERENCE

[1] Q. Zheng, J. Qi, J. Ma, P. PourMohammadi, and Q. Li, "Optically transparent wideband metamaterial absorber based on equivalent aperture and characteristic mode analysis," *Journal of Applied Physics*, vol. 135, no. 4, 2024, doi: 10.1063/5.0182434.

[2] W. Cai, P. Liu, Q. Wang, Q. Zhang, X. Pang, and W. Men, "A Double Layer Coupled Broadband Absorbing Metamaterial with Optical Transparency Characteristics," in *2023 International Applied Computational Electromagnetics Society Symposium (ACES-China)*, 15-18 Aug. 2023 2023, pp. 1-3, doi: 10.23919/ACES-China60289.2023.10249667.

[3] Y. Cui *et al.*, "Visible Transparent Wideband Microwave Meta-Absorber with Designable Digital Infrared Camouflage," *Advanced Optical Materials*, vol. 12, no. 4, p. 2301712, 2024, doi: https://doi.org/10.1002/adom.202301712.

[4] G. Deng, K. Lv, H. Sun, J. Yang, Z. Yin, B. Chi, and X. Li, "An ultra-broadband and optically transparent metamaterial absorber based on multilayer indium-tin-oxide structure," *Journal of Physics D: Applied Physics*, vol. 54, no. 16, p. 165301, 2021/02/02 2021, doi: 10.1088/1361-6463/abdb6a.

[5] R. Mirzakhani and A. Bayat, "Novel Design of Optically Transparent Circuit Analog Absorber by Modifying of exponentially tapered edge of element to achieve wider Bandwidth," (in en), *AUT Journal of Modeling and Simulation*, 2024, doi: 10.22060/miscj.2024.22964.5353.

[6] C. Xu *et al.*, *An optical-transparent flexible metamaterial for ultra-broadband microwave absorption* (Eighteenth National Conference on Laser Technology and Optoelectronics). SPIE, 2023.

[7] Y. Zhang, H. Dong, N. Mou, L. Chen, R. Li, and L. Zhang, "High-performance broadband electromagnetic interference shielding optical window based on a metamaterial absorber," *Opt. Express*, vol. 28, no. 18, pp. 26836-26849, 2020/08/31 2020, doi: 10.1364/OE.401766.

[8] Y. Zhang *et al.*, "Highly Visible–NIR Transparent Metamaterial-Window for Broadband Microwave Absorption and Shielding," *Advanced Materials Technologies*, vol. 8, no. 22, p. 2301014, 2023, doi: https://doi.org/10.1002/admt.202301014.

[9] M. Gao, Q. Chen, Y.-J. Zheng, F. Yuan, Z.-S. Sun, and Y.-Q. Fu, "Design of an optically-transparent ultra-broadband microwave absorber," *Chinese Physics B*, vol. 32, no. 8, p. 084102, 2023/08/01 2023, doi: 10.1088/1674-1056/ac9a39.

[10] S. Li, L. Liu, Y. Jiang, C. Tang, C. Gu, and Z. Li, "Ultrathin optically transparent electromagnetic shielding window with broadband microwave absorption and ultrahigh optical transmittance," *International Journal of RF and Microwave Computer-Aided Engineering*, vol. 32, no. 11, p. e23338, 2022, doi: https://doi.org/10.1002/mmce.23338.

[11] B. A. Munk, P. Munk, and J. Pryor, "On Designing Jaumann and Circuit Analog Absorbers (CA Absorbers) for Oblique Angle of Incidence," *IEEE Transactions on Antennas and Propagation*, vol. 55, no. 1, pp. 186-193, 2007, doi: 10.1109/TAP.2006.888395.

[12] K. N. Rozanov, "Ultimate thickness to bandwidth ratio of radar absorbers," *IEEE Transactions on Antennas and Propagation*, vol. 48, no. 8, pp. 1230-1234, 2000, doi: 10.1109/8.884491.

[13] C. Yang, S. Chen, S. Niu, L. Xiao, and Y.-c. Qu, "Transparent broadband microwave metamaterial absorber with thermal insulating and soundproof," *Optoelectronics Letters*, vol. 17, no. 2, pp. 85-89, 2021/02/01 2021, doi: 10.1007/s11801-021-0023-8.

[14] S. W. Tong and K. P. Loh, "3.22 - Graphene Properties and Application," in *Comprehensive Hard Materials*, V. K. Sarin Ed. Oxford: Elsevier, 2014, pp. 565-583.

[15] A. V. Mudryi, A. V. Ivaniukovich, and A. G. Ulyashin, "Deposition by magnetron sputtering and characterization of indium tin oxide thin films," *Thin Solid Films*, vol. 515, no. 16, pp. 6489-6492, 2007/06/04/ 2007, doi: https://doi.org/10.1016/j.tsf.2006.11.113.

[16] M.-J. Kim, "A Study on Optimal Indium Tin Oxide Thickness as Transparent Conductive Electrodes for Near-Ultraviolet Light-Emitting Diodes," *Materials*, vol. 16, no. 13, p. 4718, 2023. [Online]. Available: https://www.mdpi.com/1996-1944/16/13/4718.

[17] G. M. Swain, "5 - Solid Electrode Materials: Pretreatment and Activation," in *Handbook of Electrochemistry*, C. G. Zoski Ed. Amsterdam: Elsevier, 2007, pp. 111-153.

[18] R. J. Garbacz, "Modal expansions for resonance scattering phenomena," *Proceedings of the IEEE*, vol. 53, no. 8, pp. 856-864, 1965, doi: 10.1109/PROC.1965.4064.

[19] Y. Wu, H. Lin, J. Xiong, J. Hou, R. Zhou, F. Deng, and R. Tang, "A broadband metamaterial absorber design using characteristic modes analysis," *Journal of Applied Physics*, vol. 129, no. 13, 2021, doi: 10.1063/5.0043054.

[20] Z. Song, J. Zhu, L. Yang, P. Min, and F. H. Lin, "Wideband metasurface absorber (metabsorber) using characteristic mode analysis," *Opt. Express*, vol. 29, no. 22, pp. 35387-35399, 2021/10/25 2021, doi: 10.1364/OE.443182.

[21] D. Zha *et al.*, "A multimode, broadband and all-inkjet-printed absorber using characteristic mode analysis," *Opt. Express*, vol. 28, no. 6, pp. 8609-8618, 2020/03/16 2020, doi: 10.1364/OE.384954.

[22] H. Sheokand, G. Singh, S. Ghosh, J. Ramkumar, S. A. Ramakrishna, and K. V. Srivastava, "An Optically Transparent Broadband Microwave Absorber Using Interdigital Capacitance," *IEEE Antennas and Wireless Propagation Letters*, vol. 18, no. 1, pp. 113-117, 2019, doi: 10.1109/LAWP.2018.2882584.

[23] D. Systèmes. "CST Studio Suite." https://www.3ds.com/products/simulia/cst-studio-suite (accessed.

[24] M. Suo, H. Xiong, X.-K. Li, Q.-F. Liu, and H.-Q. Zhang, "A flexible transparent absorber bandwidth expansion design based on characteristic modes," *Results in Physics*, vol. 46, p. 106265, 2023/03/01/ 2023, doi: https://doi.org/10.1016/j.rinp.2023.106265.

[25] A. Bayat and R. Mirzakhani, "A parametric study and design of the balanced antipodal Vivaldi antenna (BAVA)," presented at the PIERS (Progress In Electromagnetics Research), Moscow, Aug,19,2012, 2012, 778-782. [Online]. Available: https://www.piers.org/pierspublications/PIERS2012MoscowProceedings02.pdf.